# Synthesis and Bulk, Surface, and Microlithographic Characterization of Poly(1-butene sulfone)-g-poly(dimethylsiloxane)

**J. M. DeSimone,† G. A. York,‡ and J. E. McGrath***

*Department of Chemistry, NSF Center for High Performance Polymeric Adhesives and Composites, Virginia Polytechnic Institute and State University, Blacksburg, Virginia 24061*

**A. S. Gozdz and M. J. Bowden**

*Bell Communications Research, Red Bank, New Jersey 07701*

*Received March 29, 1991; Revised Manuscript Received May 3, 1991*

ABSTRACT: Hexenyl-functionalized poly(dimethylsiloxane) (PDMS) macromonomers were synthesized by the anionic ring-opening polymerization of hexamethylcyclotrisiloxane. These macromonomers were terpolymerized under free-radical conditions with 1-butene and sulfur dioxide to form the title graft copolymers. The molar masses of the macromonomers were varied from 1K to 20K g/mol, and the copolymer compositions ranged from 5 to 20 wt % PDMS. The bulk and surface phase morphologies were investigated by using DSC, TEM, XPS, and water contact angle measurements. The graft copolymers were evaluated as electron-beam resists; their sensitivity was ca. 4.5 $\mu C/cm^2$ at 25 kV, and their etch rate ratio during oxygen reactive ion etching relative to a cross-linked novolac resin was 1:29.

## Introduction

Alternating copolymerization is one of the most interesting areas in free-radical polymerizations. In particular, the alternating copolymerization of various olefins with sulfur dioxide has generated significant interest.[1] The resultant poly(olefin sulfone)s are noted for their susceptibility to degradation upon exposure to high-energy radiation such as $\gamma$-rays and electrons.[2] Indeed, workers in the field of lithography have exploited the inherently labile nature of these polymers and have demonstrated the important technological aspect of the poly(olefin sulfone)s as electron beam resists.[3]

In the early 1980s, the aerospace industry showed that the degradation and weight loss observed when organic polymers are placed in low-earth orbit (where an abundance of aggressive atomic oxygen exists) could be dramatically reduced by incorporating certain refractory elements into the polymer.[4-6] For example, the incorporation of poly(siloxane)s into high-performance materials such as poly(imide)s and poly(benzimidazole)s greatly extends the utility of these materials in a variety of specialty aerospace applications.[7] Since the mid-1970s, researchers in the area of microlithography have been exploring this idea of incorporating refractory elements into organic polymers to improve resistance to oxygen reactive ion etching (RIE). Studies showed that, by incorporating elements such as silicon or titanium into organic polymers, the oxygen RIE resistance of the resultant polymers could be significantly enhanced.[8] This work subsequently led to the development of a variety of multilevel[8a] resist materials and processes for fabricating devices with submicron resolution. Some examples of silicon-containing poly(olefin sulfone)s investigated in our laboratories include poly(3-butenyltrimethylsilane sulfone),[9] poly[(trimethylsilyl)styrene sulfone],[10,11] and poly(methyl methacrylate)-g-poly(dimethylsiloxane).[12]

Recently, we reported the synthesis of poly(norbornene sulfone)-g-poly(dimethylsiloxane)[13] using terminally unsaturated poly(dimethylsiloxane) (PDMS) as a macromonomer. We report here the detailed synthesis, physical characterization, and lithographic evaluation of a related material, poly(1-butene sulfone)-g-poly(dimethylsiloxane) (PBS-g-PDMS). By incorporating silicon in the form of microphase-separated PDMS grafts, as opposed to molecularly dispersed or homogeneous $-SiR_3$ moieties, we hoped to improve the oxygen RIE resistance as a result of enhanced surface domination of PDMS due to its low surface free energy while retaining the high sensitivity toward electron beam irradiation of the poly(olefin sulfone). In addition, the multiphase graft copolymers should have different solubility characteristics with respect to the single-phase materials, thus allowing a wider window of development conditions relative to poly($\omega$-alkenyltrimethylsilane sulfone)s.

## Experimental Section

**Reagents.** Cyclohexane (Fisher; reagent grade) was stirred over concentrated sulfuric acid for ca. 2 weeks, decanted, and distilled under nitrogen from a sodium dispersion. Tetrahydrofuran (THF; Fisher; certified grade) was distilled under nitrogen from the purple sodium/benzophenone ketyl. Dichloromethane (Mallinckrodt; analytical grade) was fractionally distilled from calcium hydride under nitrogen. Hexamethylcyclotrisiloxane ($D_3$) was generously provided by General Electric. The cyclic monomer was melted, stirred over finely divided calcium hydride under nitrogen for ca. 12 h, and then sublimed under vacuum. The sublimed monomer was then dissolved in purified cyclohexane to obtain a stock solution of ca. 43 w/v %, which was stored under nitrogen. 5-Hexenyldimethylchlorosilane (HDMCS) (Petrarch), 1-butene (Aldrich), sulfur dioxide (Aldrich; anhydrous grade), *tert*-butyl hydroperoxide (TBHP; Aldrich; 90 w/v % in isopropyl alcohol diluted to 0.016 g/mL with degassed dichloromethane), triethylamine (Aldrich), chloroform (Aldrich), and *sec*-butyllithium (generously supplied by Lithco) were used as received. Cyclopentanone (Aldrich) was purified by passing it through a column of neutral alumina.

**PDMS Macromonomer Synthesis.** Anionic polymerizations were carried out in rigorously cleaned and dried one-neck round-bottomed flasks equipped with magnetic stir bars and rubber septa under a 6-8 psig nitrogen atmosphere. In a typical polymerization, the cyclohexane solution of $D_3$ was syringed into the reaction flask followed by a calculated amount of 1.35 M *sec*-butyllithium to initiate the ring-opening polymerization. The initiation reaction was allowed to proceed for ca. 2 h, at which

* Author to whom correspondence should be addressed.
† Present address: Venable and Kenan Laboratories, Department of Chemistry, CB 3290, The University of North Carolina at Chapel Hill, Chapel Hill, NC 27599-3290.
‡ Present address: Shell Development Co., P.O. Box 1380, Houston, TX 77251-1380.

0024-9297/91/2224-5330$02.50/0 

point sufficient purified THF was added to give a 10 v/v % solution to promote propagation of the living siloxanolate anion. The polymerization was terminated after 48 h with HDMCS, and the macromonomer was precipitated in methanol, washed three times with methanol, and dried to constant weight under reduced pressure at room temperature. The PDMS macromonomers were characterized by $^1$H NMR (Bruker WP 270 in $CDCl_3$), $^{29}$Si NMR (Bruker WP 200 in 0.4 M chromium(III) acetylacetonate in $CDCl_3$, inverse-gated pulse program), and GPC (Waters 590 GPC with Ultrastyragel columns of 100-, 500-, $10^3$-, and $10^4$-Å porosities in toluene using PDMS GPC standards synthesized and characterized in our laboratories).

**Synthesis of PBS-g-PDMS.** The free-radical terpolymerizations of 1-butene, sulfur dioxide, and the PDMS macromonomers were carried out in a modified Fisher–Porter bottle that was equipped with an in-house machined reactor cap containing a vacuum inlet, a nitrogen inlet, a septum port, a thermocouple, a cooling coil, and an overhead motor-driven Parr stirrer.

The required amount of 5-hexenyl-terminated PDMS macromonomer was charged to the Fisher–Porter polymerization reactor, which was then assembled to the reactor cap. The PDMS macromonomer was thoroughly degassed under vacuum at room temperature for 30 min. After degassing, the reactor was backfilled with nitrogen and the polymerization solvent, dichloromethane, was added via syringe in an amount corresponding to a 20 w/v % solution of total polymer in dichloromethane. The reactor was cooled to the polymerization temperature of −20 °C by manually controlling the amount of liquid nitrogen passing through the cooling coil. The required amounts of 1-butene and sulfur dioxide were condensed into separate calibrated vessels and transferred via cannula into the stirred polymerization reactor. The free-radical initiator, TBHP, was added via syringe. Two series of graft copolymers were synthesized: a low degree of polymerization (low-$\bar{X}_n$) series and a high degree of polymerization (high-$\bar{X}_n$) series. The low-$\bar{X}_n$ series was prepared by using 1.7 w/w % (based on 1-butene and sulfur dioxide) of TBHP, and the high-$\bar{X}_n$ series was prepared by using 0.4 w/w % TBHP, which was added over a 20-min period in 0.1 w/w % aliquots at 5-min intervals. The resulting graft copolymers were precipitated 20 min after initiation into a 10-fold excess of methanol containing 2 v/v % triethylamine, filtered, and dried to constant weight under reduced pressure at room temperature. The polymers were extensively extracted with hexanes in a Soxhlet extractor to remove any unincorporated PDMS macromonomer. The extracted polymers were routinely stored at −20 °C. The compositions of the graft copolymers were determined by $^1$H NMR (Bruker WP 270). Intrinsic viscosities were determined in dichloromethane at 25 °C by a Cannon CUU 50 Ubbelohde capillary viscometer.

**Morphological Characterization.** The morphology of the graft copolymers was investigated by differential scanning calorimetry (DSC) and transmission electron microscopy (TEM). DSC thermograms were obtained on a Seiko Instruments System I DSC 210. The neat PDMS oligomers were quenched to −160 °C and heated to 0 °C at 5 °C/min. The PBS-g-PDMS copolymers were analyzed as precipitated powders (5–7 mg). Samples were initially heated above their glass transition temperatures ($T_g$) to 120 °C, annealed at 120 °C for 10 min, and then quickly quenched to −160 °C. The samples were then heated to 120 °C at 5 °C/min. Glass transitions were determined as the midpoint of the change in heat capacity, $\Delta T_g$ is the difference in temperature between the point at which the DSC trace first deviated from the base line and the temperature corresponding to the maximum of the physical aging peak. The percent crystallinity was determined by

$$\% \text{ crystallinity} = (\Delta H_m/\Delta H_m^\circ) \times 100$$

where $\Delta H_m$ is the experimentally measured heat of fusion of the sample, and $\Delta H_m^\circ$ is the heat of fusion of a perfectly crystalline material. The value of $\Delta H_m^\circ$ for PDMS has been reported[14,15] to be 61.19 mJ/mg, which was obtained from melting point depression data. Films of the PBS-g-PDMS copolymers were prepared for TEM analysis by casting dilute chloroform solutions (2.5 w/v %) of the copolymers in glass vials or Petri dishes and allowing the solvent to evaporate slowly (ca. 48 h). The films were sectioned on a Reichert–Jung Ultracut FC-4 ultramicrotome system using a diamond knife at a temperature of about −110 °C with the specimens floating on methanol. A Philips EM 420 TEM operating at 100 kV was utilized for the TEM analysis with condenser and objective apertures of 50 and 30 μm, respectively. The contrast between the two components of the graft copolymer was sufficient enough to preclude the need for any staining procedures.

**Surface Analysis.** Films of the low-$\bar{X}_n$ PBS-g-PDMS copolymers were prepared for surface analysis by casting dilute chloroform solutions of the copolymers onto metal plates in glass-covered Petri dishes and allowing the solvent to evaporate slowly (ca. 48 h). The substrates, coated with the graft copolymer, were placed in the goniometer at room temperature and at atmospheric conditions. Distilled water was added dropwise in 0.002-mL increments until an equilibrium contact angle (the advancing contact angle) was measured. The drop was subsequently removed in similar increments, and the contact angle was measured until an equilibrium contact angle (the receding contact angle) was established. This procedure was repeated 3–4 times at various locations on the film surface in order to ensure uniformity of structure, and all values reported in this paper represent the average of several readings. Agreement was generally within ±2°. Angular-dependent X-ray photoelectron spectroscopy (ADXPS) was carried out on a KRATOS XSAM 800 spectrometer equipped with a hemispherical electron analyzer and a magnesium X-ray source operated at 15 kV and 20 mA. Angle-dependent analysis over the range of 10–90° was performed by rotating the sample probe. The PBS-g-PDMS copolymers were cooled to ca. −120 °C to avoid degradation of the sample during analysis. Surface topography generated by exposure of the films to oxygen RIE was studied by using a Philips EM 420 STEM operating in the SEM mode. Samples were coated with 10–30 nm of gold to minimize charging effects.

**Lithographic Processes and Measurements.** The title graft copolymers were dissolved in cyclopentanone to yield 5 w/w % solutions. Graft copolymers having 20K grafts were dissolved in chloroform because of the insolubility of these materials in the cyclic ketone. Pure novolac resin (1.2-μm-thick film, spin-coated from 10 w/w % ethoxyethyl acetate and cross-linked by heating at 200 °C for 1 h) was used as the bottom layer in a two-layer resist system cn a silicon substrate. All solutions were filtered through 0.45-μm filters. The resistance of the graft copolymers to oxygen RIE was determined on ca. 2200-Å-thick films. The oxygen RIE resistance was determined by using a Cooke Vacuum Products parallel-plate reactor at a radio frequency of 13.56 MHz, 15 mTorr oxygen pressure, a flow rate of 10 sccm, and a self-bias of −350 V. Films of known initial film thickness were withdrawn from the oxygen RIE chamber at varying time intervals and their thicknesses monitored as a function of etch time using a surface profilometer (Tencor Instruments, Alpha Step 200). Sensitivity curves were established on the two-layer test samples. A PBS-g-PDMS film was spin-coated onto a silicon wafer that had been precoated with a cross-linked novolac film and prebaked for 15 min at 110 °C. The resulting graft copolymer layer was 1800 Å thick. Lithographic sensitivity and resolution tests have been carried out by exposing resist samples with an electron beam at 25 and 50 kV, respectively, using a JEOL JBX II(U) instrument. The exposed patterns were dip-developed in 5-methyl-2-hexanone at 16–23 °C for 30–60 s, rinsed for 5 s in 2-propanol, and dried in a stream of air. The film thickness remaining after development in each exposed area was measured with the profilometer, and the results were plotted as normalized film thickness vs log (dose). Patterns developed in the PBS-g-PDMS top layer were transferred into the bottom layer by 14 min of oxygen RIE by using the RIE system and the procedure described above.

## Results and Discussion

**Graft Copolymer Synthesis and Molecular Characterization.** The parameters that effect the ability or efficiency of a macromonomer to copolymerize with other monomers are numerous, the most important being the nature of the substitution at the polymerizable end group of the macromonomer. In order to incorporate the PDMS

**Scheme I**
**Synthesis of Poly(dimethylsiloxane) Macromonomers**

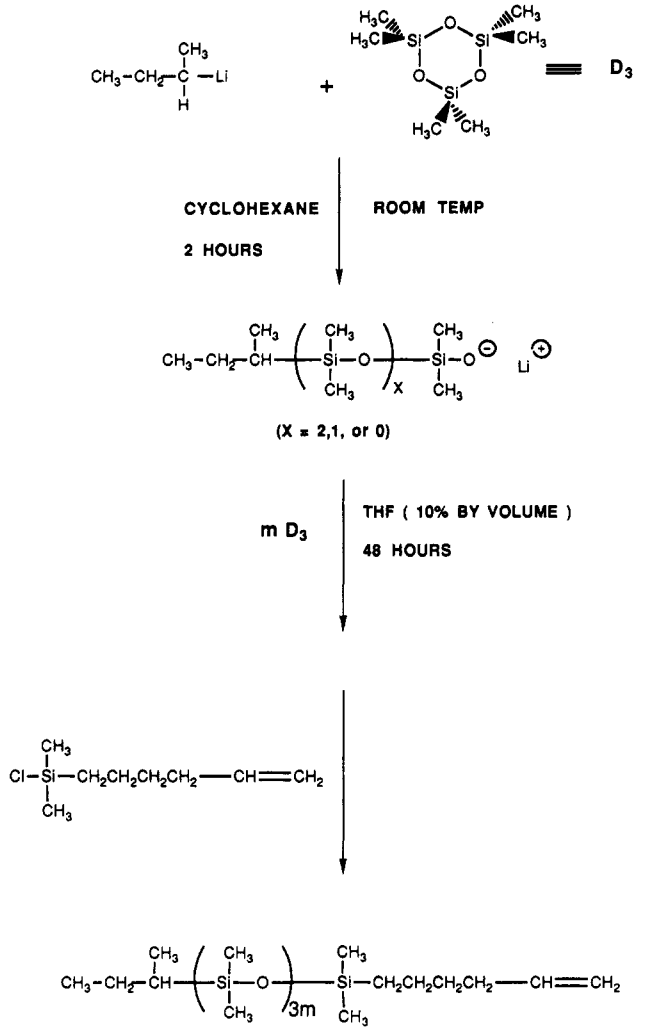


macromonomers into PBS in a statistical fashion, it was necessary to design the macromonomer to have an end group closely emulating 1-butene.

The preparation of the 5-hexenyl-functionalized PDMS macromonomers of high functionality, controlled molar mass, and narrow molar mass distribution was the first step in preparing well-defined graft copolymers. The synthesis of the macromonomers is outlined in Scheme I. The addition of *sec*-butyllithium to the pure cyclohexane solution of $D_3$ results in the initiation of the polymerization without any subsequent propagation, on account of the fact that, in nonpolar solvents such as cyclohexane, the living siloxanolate exists as a very tight ion pair[16] with no dissociation to form free ions. These ion pairs, in turn, exist as aggregates of four ion pairs.[17] Upon the addition of a polar "promoting" solvent, such as THF, the tight ion pairs shift to loose ion pairs (THF probably also breaks up the ion-pair aggregates to some extent), thereby allowing propagation to occur. In the absence of termination and chain-transfer reactions, polymerization proceeds in a living manner.[18-23] After 48 h, the polymerization was terminated with HDMCS, yielding the 5-hexenyl-functionalized macromonomer. We have shown, by $^{29}Si$ NMR,[24] GPC, and end-group analysis by FTIR[25] that even toward the end of the polymerization reaction, under the times and conditions used here, no cyclic formation and no broadening of the molar mass distribution occur. This procedure allows excellent control of the molar mass, the molar mass distribution, and the functionality of the

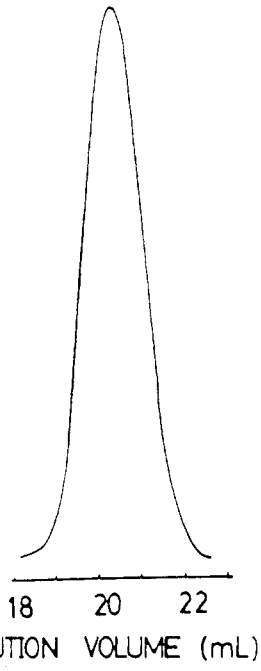


**Figure 1.** GPC trace of poly(dimethylsiloxane) macromonomer.

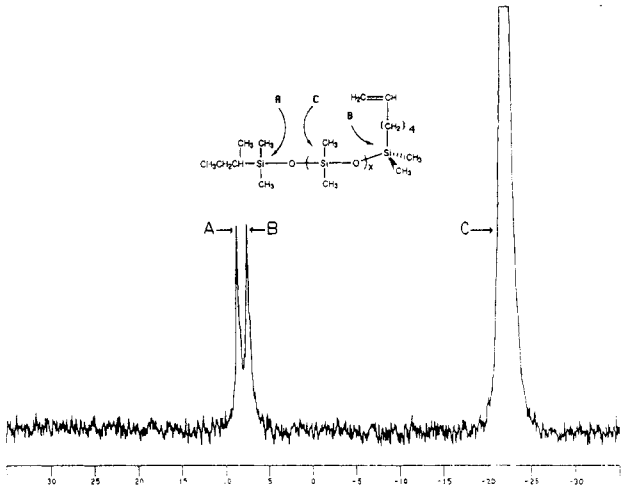


**Figure 2.** Quantitative $^{29}Si$ NMR spectrum of hexenyl-functionalized 1K g/mol PDMS macromonomer.

PDMS macromonomers. The molar mass of the polymer was controlled simply by the ratio of the grams of the $D_3$ monomer and the moles of initiator with target molar masses of 1K, 5K, 10K, and 20K g/mol. The molar mass and the molar mass distribution of the PDMS macromonomers were determined by GPC calibrated with PDMS standards (Figure 1).

The number-average molar mass and the functionality of the macromonomers were determined by using $^{29}Si$ NMR. Model compounds were utilized to make the assignments. As can be seen in Figure 2, there are three different types of silicon atoms present in the PDMS macromonomers. The NMR technique can differentiate between the silicon atoms next to the initiating *sec*-butyl fragment and the terminating 5-hexenyl fragment and in the repeating dimethylsiloxane unit. The ratio of the integration of the repeating silicon atoms to that of an end group gives the number-average molar mass while the ratio of the integration of the terminal silicons results in a direct determination of the percent functionality of the PDMS macromonomers. The results of the GPC and $^{29}Si$ NMR analyses are given in Table I, along with the target molar

**Table I**
**Summary of Molecular Characterization of PDMS Macromonomers**

| theor $\langle M_n \rangle$, g/mol | $\langle M_n \rangle$,[a] g/mol | $\langle M_n \rangle$,[b] g/mol | $\langle M_w \rangle / \langle M_n \rangle$[b] | functional,[a] % |
|---|---|---|---|---|
| 1K | 940 | | | 100 |
| 5K | 5600 | 4100 | 1.08 | 100 |
| 10K | 9800 | 7200 | 1.05 | 100 |
| 20K | 24600 | 17500 | 1.03 | 94 |

[a] $^{29}$Si NMR. [b] GPC with PDMS standards.

**Scheme II**
**Synthesis of PBS-g-PDMS**

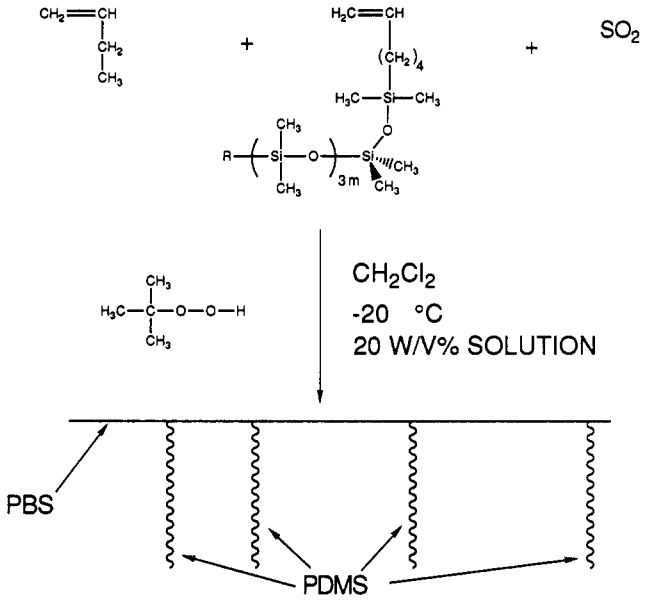


masses for the macromonomers. As one can see, the experimental results correlate well with the target values.

Terpolymerizations of the 5-hexenyl-functionalized PDMS macromonomer with 1-butene and sulfur dioxide were carried out such that the number-average molar masses of the macromonomers and the compositions of the graft copolymers were both varied. This ability to keep the copolymer composition constant while changing the length of the graft incorporated enables the architecture of the system to be changed at constant composition. The free-radical terpolymerizations, shown in Scheme II, needed to be carried out in dilute solution (20 w/v %). At higher concentrations, macrophase separation occurred as evidenced by the onset of cloudiness during the terpolymerization; however, at concentrations at 20 w/v % or lower, the terpolymerizations remained clear throughout the course of the reaction.

Once the polymers were precipitated, the unincorporated PDMS macromonomer was removed from the graft copolymer by thorough extraction with hexanes in a Soxhlet extractor. Films of the graft copolymers were cast from samples before and after extraction. Samples that were not extracted gave cloudy films, and samples that were thoroughly extracted resulted in clear films. A typical $^1$H NMR spectrum of a purified PBS-g-PDMS is shown in Figure 3. The compositions were determined by ratioing the integrated signal intensity of the silicon methyl resonance at 0.1 ppm to the methylene and methine signals of the PBS component. The compositions of the graft copolymers are presented in Table II along with the corresponding initial feed ratios. In addition, the copolymers are grouped into categories based on the composition and degree of polymerization (high, low) as shown. The

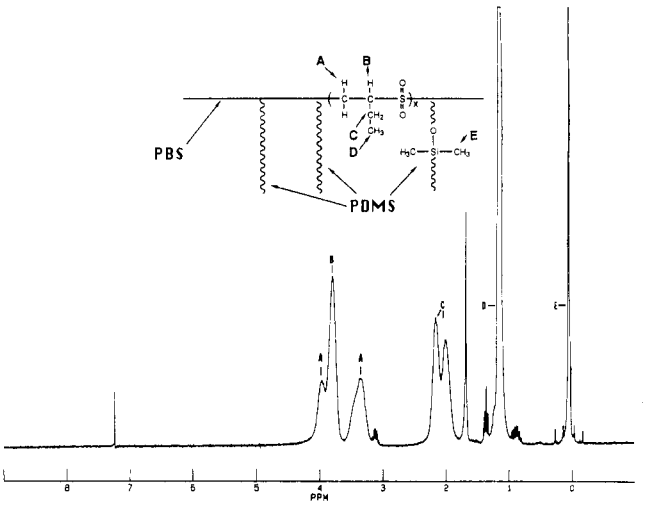


**Figure 3.** $^1$H NMR spectrum of the low-$\bar{X}_n$ PBS-g-PDMS having 6 wt % of 5K g/mol PDMS grafts.

**Table II**
**Summary of PBS-g-PDMS Copolymer Synthesis and Series Designation**

| sample | PDMS $\langle M_n \rangle$, g/mol | PDMS charged, wt % | PDMS inc.,[a] wt % | series designations: PDMS composn, wt % | |
|---|---|---|---|---|---|
| 026-A | 1K | 9 | 6 | | |
| 026-B | 5K | 9 | 6 | | |
| 026-C | 10K | 9 | 6 | 6 | |
| 026-D | 20K | 9 | 7 | | low $\bar{X}_n$ |
| 017-A | 1K | 29 | 23 (21) | | |
| 017-B | 5K | 29 | 20 (20) | | |
| 017-C | 10K | 29 | 20 (23) | 20 | |
| 017-D | 20K | 29 | 17 (19) | | |
| 031-A | 1K | 9 | 5 | | |
| 031-B | 5K | 9 | 5 | | |
| 031-C | 10K | 9 | 5 | 5 | |
| 031-D | 20K | 9 | 6 | | high $\bar{X}_n$ |
| 029-A | 1K | 29 | 19 | | |
| 029-B | 5K | 29 | 19 | | |
| 029-C | 10K | 29 | 17 | 17 | |
| 029-D | 20K | 29 | 15 | | |

[a] Values obtained by $^1$H NMR analyses of extracted graft copolymers. Values in parentheses were determined by differential refractometry.

formalism indicated will be used throughout the paper. As one can see, approximately 65% of the PDMS charged was actually incorporated into the copolymer. While the percent of PDMS macromonomer incorporated may seem rather low, it is not due to unfunctionalized PDMS macromonomer as shown earlier; however, it can be rationalized on the fact that the solubility parameter of PDMS is very different from that of PBS. It has been shown[26] that when the macromonomer is chemically different from the backbone material, there is a tendency toward lowering of the macromonomer incorporation efficiency. The difference between the solubility parameters of PDMS and PBS is quite large, on the order of 2.7 $(cal/cm^3)^{1/2}$, which would account for the lower incorporation efficiency of the macromonomer in this system.

The compositions listed in Table II were determined by $^1$H NMR as described earlier. The four values listed in parentheses for the low-$\bar{X}_n$, 20 wt % PDMS series were determined by differential refractometry[27] in methyl ethyl ketone. The compositions obtained by the different methods correlate well with one another. This correlation gives credibility to the data obtained by $^1$H NMR, which

**Table III**
**Summary of Molar Mass Characterization of PBS-*g*-PDMS**

| sample | compsn of PDMS, wt % | intrinsic viscosity,[a] dL/g | $\langle M_{w,apparent} \rangle$, g/mol | $\langle M_{w,backbone} \rangle$,[c] g/mol |
|---|---|---|---|---|
| 026-A | 6 | 0.06 | | |
| 026-B | | 0.12 | | |
| 026-C | | 0.14 | | |
| 026-D | | 0.27 | | |
| 017-A | 20 | 0.04 | 68K | 54K |
| 017-B | | 0.09 | 50K | 40K |
| 017-C | | 0.18 | 47K | 37K |
| 017-D | | 0.14 | 41K | 32K |
| 031-A | 5 | 0.16 | | |
| 031-B | | | | |
| 031-C | | | | |
| 031-D | | | | |
| 029-A | 17 | 0.29 | | |
| 029-B | | 0.24 | | |
| 029-C | | 0.28 | | |
| 029-D | | 0.28 | | |

[a] Dichloromethane, 25 °C. [b] Calculated based on isorefractive light scattering data: $\langle M_{w,backbone} \rangle = \langle M_{w,apparent} \rangle (1 - X_{PDMS})$, where $X_{PDMS}$ is the weight fraction PDMS in the copolymer. [c] Isorefractive light scattering in THF at 25 °C.

can be complicated by micellularization problems that often occur with block and graft copolymers.

**Bulk and Surface Characterization. Molar Mass.** The molar masses of the graft copolymers were investigated by using intrinsic viscosity measurements, which were supplemented in a few cases with apparent weight-average molar masses measured in Professor Kratochvil's laboratory using isorefractive light scattering techniques.[27] The values, listed in Table III, show that the low-$\bar{X}_n$ copolymers have very low intrinsic viscosities ranging from 0.06 to 0.18 dL/g. However, the corresponding apparent weight-average molar masses, $\langle M_{w,apparent} \rangle$, range from 68K to 41K g/mol, which decrease as the graft molar mass increases. In addition, the weight-average molar mass for the PBS component, $\langle M_{w,backbone} \rangle$, obtained by isorefractive light scattering in THF, shows that the molar mass of the PBS backbone also decreases as the molar mass of the graft increases. These unusual and unexpected trends in the molar mass of the copolymers as a function of graft molar mass are under investigation. This may indicate that, during the synthesis, the system is beginning to phase separate to a degree that is not detectable to the eye and therefore is affecting the incorporation of the macromonomer or the growing macroradical's reactivity.

**Thermal Analysis.** Glass transition temperature and crystallization measurements can yield valuable information on the degree of phase separation in multicomponent systems. For graft copolymers prepared by the macromonomer method, much can be learned by comparing the thermal transitions of the macromonomer in its neat form and after its incorporation into a graft copolymer. The properties that were investigated in this study include measurement of the glass transition temperature of the corresponding homopolymers of PDMS and PBS and the crystallization characteristics of PDMS. The results on the homopolymers were then compared to the analogous transitions for the graft copolymers.

**Neat PDMS Macromonomer DSC Results.** DSC thermograms were obtained on the four different molar mass PDMS macromonomers. Figures 4 and 5 show the DSC thermograms for the 20K g/mol macromonomer corresponding to two different thermal cycles. Figure 4 is a composite graph showing the dynamics of the experiment. The instrument response to the thermally induced transitions is plotted on the left $y$ axis, and temperature is plotted on the right $y$ axis. Time is plotted on the $x$ axis. As shown in Figure 4, the sample was rapidly cooled to a crystallization temperature of −72 °C (from 0 to 15 min), isothermally crystallized for 30 min (from 15 to 45 min), and slowly heated (from 45 to 60 min). Crystallization is shown to begin shortly after reaching −72 °C, as evidenced by the crystallization exotherm. Upon heating, a relatively narrow melting endotherm is then observed at ca. −42 °C. Figure 5 shows the DSC thermogram for the same 20K g/mol PDMS macromonomer; however, the thermogram represents a conventional heating curve obtained after previously quenching the sample to −150 °C. A comparison of the melting transition of PDMS in Figure 5 with the portion of Figure 4 representing the melting of PDMS after isothermal crystallization (from 45 to 60 min) shows that there are significant differences between the two thermograms reflecting the different thermal histories. The region between −80 and −20 °C has been expanded for the quenched sample and is shown in Figure 6. A large cold crystallization exotherm, $T_c$, exists beginning immediately after reaching the glass transition temperature followed by several reproducible and rather well-defined endothermic transitions prior to the larger melting transitions usually associated with PDMS.[28] The dependence of these small transitions on heating rate suggests that they may be due to lamellae thickening or reorganization of metastable crystals during heating. We are currently investigating this phenomenon in greater detail.

The percent crystallinity of the neat PDMS macromonomers was calculated as described in the Experimental Section. The DSC results for the neat PDMS macromonomers are shown in Table IV. The macromonomers with

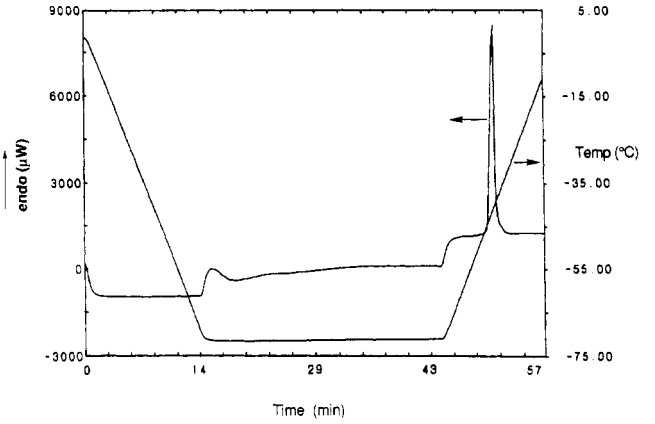


**Figure 4.** Typical isothermal crystallization DSC experiment for PDMS.

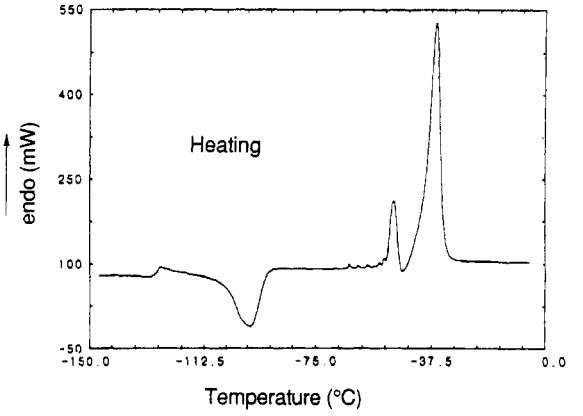


**Figure 5.** DSC thermogram for quenched PDMS macromonomer.

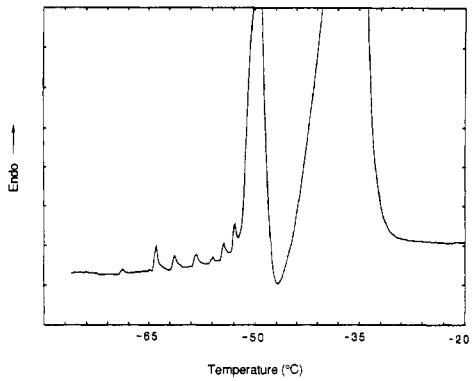


**Figure 6.** Expanded DSC thermogram for quenched PDMS showing multiple endotherms.

**Table IV**
**Summary of DSC Characterization of Neat PDMS Macromonomers**

| macromonomer, g/mol | $T_g$, °C | $T_m$, °C | $T_c$, °C |
|---|---|---|---|
| 1K | -135 | | |
| 5K | -130 | | |
| 10K | -129 | -49/-35 | -88 |
| 20K | -126 | -50/-35 | -97 |

**Table V**
**Summary of DSC Characterization of PBS-g-PDMS Copolymers**

| PBS-g-PDMS high $\bar{X}_n$ | PDMS | | | PBS | |
|---|---|---|---|---|---|
| | $T_g$, °C | $T_m$, °C | cryst, % | $T_g$, °C | $\Delta T_g$, °C |
| 17 wt %, 1K PDMS | | | | 80 | 20 |
| 17 wt %, 5K PDMS | | -60 | 13 | 86 | 17 |
| 17 wt %, 10K PDMS | | -48 | 15 | 91 | 12 |
| 17 wt %, 20K PDMS | | -42 | 11 | 92 | 12 |
| PBS control | NA | NA | NA | 92 | 12 |

molar masses greater than 5K g/mol exhibited multiple melting endotherms and crystallization exotherms depending on their mode of cooling. The lowest molar mass PDMS macromonomer, 1K g/mol, was not observed to crystallize under these conditions. The $T_g$ of the PDMS macromonomer increased as the molar mass increased, reflecting the dependence of the glass transition on molar mass in this low molar mass region.

**PDMS Crystallization in Graft Copolymer.** When the PBS-g-PDMS copolymers were subjected to conditions identical with those of the neat PDMS isothermal crystallization experiments, only weak PDMS melting transitions were observed. The results indicate that less than 1% of the PDMS component had crystallized in the copolymer whereas the neat PDMS macromonomers developed 30% to 50% crystallinity under the same conditions. The inability of the grafted PDMS to achieve high levels of crystallinity under these identical conditions reflects the constraints that accompany incorporation of oligomers into a multicomponent material. Larger and more quantifiable melting endotherms were measured, however, when the samples were quick-quenched to -150 °C and then heated as previously described.

**Comparison of Homopolymer and Graft Copolymer DSC Results.** A summary of the DSC results for the graft copolymers is shown in Table V. No detectable PDMS $T_g$ was observed for the high-$\bar{X}_n$ PBS-g-PDMS copolymers having 17 wt % PDMS regardless of the molar mass of the PDMS graft. Single-melting endotherms were observed for the PDMS component in all of the PBS-g-PDMS graft copolymers having 17 wt % PDMS except the graft copolymer with 1K g/mol PDMS grafts (which was observed not to crystallize even in its neat form). A shift in the melting temperature ($T_m$) of the PDMS component to higher temperatures with increasing graft molar mass was observed. This may indicate an increase in the degree of microphase separation with an increase in the molar mass of the PDMS graft. The percent crystallinity of the PDMS component, also shown in Table V, did not appear to be a function of the graft molar mass. This may be due to a change in morphology and will be discussed later in the section dealing with TEM. A parallel shift in the $T_g$ and the $\Delta T_g$ of the PBS component was observed. The PBS $T_g$ increases and the $\Delta T_g$ decreases with a corresponding increase in the molar mass of the PDMS grafts and begins to approach the values measured for pure PBS. This trend possibly indicates a decrease in the degree of phase mixing between the two components with an increase in the graft molar mass.

The reason that the above data only *possibly* indicate a change in the degree of phase mixing with graft molar mass is due to the corresponding topology change that also occurs when the graft molar mass is changed. The change in topology results in changes in the molar mass between branch points for the backbone component. It is the molar mass between branch points that is the effective portion of the backbone component that is in the PBS-rich phase and therefore experiences the influence of the critical molar mass for chain entanglements on its ability to undergo a transition from the glassy state to the rubbery state. This reflects the nature of the morphology, which places the branch points at the interface of the different phases. The forced constraint of locating the branch points at the interface surely alters their ability to entangle, relative to a homopolymer of equal $\bar{X}_n$, and therefore may influence the $T_g$ measurements. A theoretical analysis on the effect of the number of junction or branch points in graft copolymers coupled with experimental evaluation is encouraged.

The driving force for phase separation in block and graft copolymers derives from the difference in solubility parameters between the two components. Given the large disparity between the solubility parameters of PDMS, 7.3 $(cal/cm^3)^{1/2}$, and PBS, 10 $(cal/cm^3)^{1/2}$, we would have expected that the graft copolymers would be sharply phase separated. An interesting comparison can be made between the PBS-g-PDMS copolymers and poly(methyl methacrylate)-g-poly(dimethylsiloxane) copolymers.[25] The solubility parameter for PMMA is 9.1 $(cal/cm^3)^{1/2}$, almost a full unit less than that for PBS without even including the larger polar contribution of PBS not accounted for in the Hildebrand solubility parameters. We would therefore predict a higher degree of phase mixing in PMMA-g-PDMS than we would for the PBS-g-PDMS system at equivalent degrees of polymerization, composition, and topology. This prediction is confirmed since the earlier study showed that the PDMS component in the PMMA-g-PDMS copolymers having the same weight percent PDMS and graft molar mass as the PBS-g-PDMS listed in Table IV was not able to crystallize under similar thermal treatments.[25]

**Electron Microscopy.** TEM analysis demonstrated that the morphology of the PBS-g-PDMS system depends markedly on copolymer composition and architecture. The overall degree of polymerization at constant compositions and architectures had a particularly marked effect. Both the low-$\bar{X}_n$ and high-$\bar{X}_n$ copolymers having 5 wt % PDMS exhibited discrete morphologies with spherical PDMS domains in a continuous PBS matrix as shown in the top portions of Figures 7 and 8. The domain sizes increase with a corresponding increase in the molar mass of the

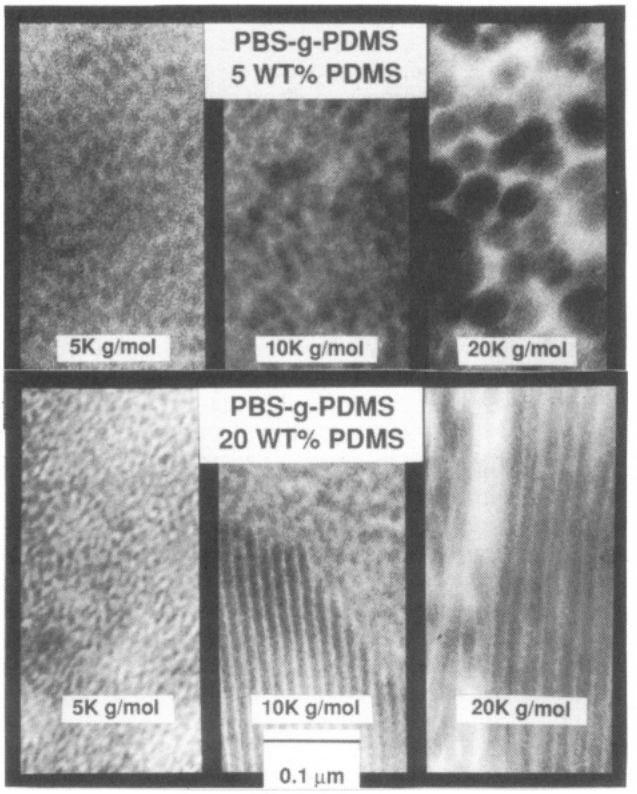


**Figure 7.** TEMs of low-$\bar{X}_n$ PBS-*g*-PDMS copolymer having 5 and 20 wt % PDMS with PDMS molar masses of 5K, 10K, and 20K g/mol.

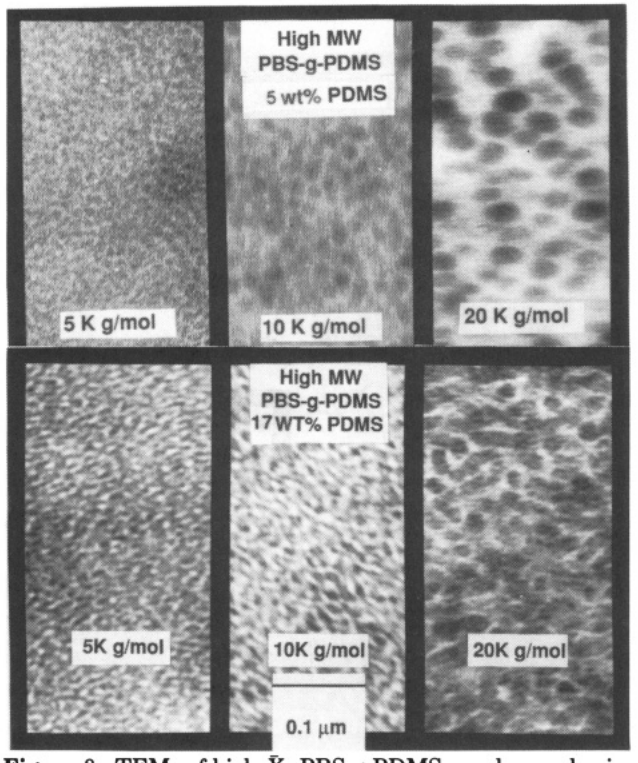


**Figure 8.** TEMs of high-$\bar{X}_n$ PBS-*g*-PDMS copolymers having 5 and 17 wt % PDMS with PDMS molar masses of 5K, 10K, and 20K g/mol.

PDMS graft at constant composition. At 20 wt % PDMS, the low-$\bar{X}_n$ copolymers exhibit semicontinuous morphologies (see bottom portion of Figure 7). The low-$\bar{X}_n$, high weight percent siloxane PBS-*g*-PDMS copolymer with 5K g/mol PDMS grafts shows a disordered bicontinuous morphology whereas the copolymers with 10K and 20K g/mol PDMS grafts show ordered cylindrical or lamellar morphologies with regions of disorder. The high-$\bar{X}_n$, high weight percent siloxane graft copolymers with 5K and 10K g/mol PDMS grafts exhibit bicontinuous disordered morphologies (see bottom portion of Figure 8) while the copolymer with 20K g/mol PDMS grafts exhibits a broken cylindrical or lamellar morphological texture. The low-$\bar{X}_n$ and high-$\bar{X}_n$ copolymers with 10K and 20K g/mol grafts containing high concentrations of siloxane exhibit very different morphologies. These morphological differences can be attributed to the differences in the number of branch or junction points per molecule as the overall degree of polymerization is changed. The low-$\bar{X}_n$ copolymers have fewer junction points per molecule than do the high-$\bar{X}_n$ copolymers. These junction points need to be placed at the interphase region between the PBS-rich phases and the PDMS-rich phases. These entropic constraints decrease the degrees of freedom for the high-$\bar{X}_n$ copolymers, inhibiting the ability of the backbone to uniformly fill in domain spaces since they have more branch points per molecule than do the low-$\bar{X}_n$ copolymers, therefore disrupting packing, resulting in disordered morphologies.

**Table VI**
**Advancing and Receding Water Contact Analyses of Low-$\bar{X}_n$ PBS-*g*-PDMS Copolymers Having 5 and 20 wt % PDMS with 1K, 5K, 10K, and 20K g/mol PDMS Grafts**

| sample | water contact angle | |
|---|---|---|
| | advancing | receding |
| PBS | 73 | 48 |
| PDMS (cross-linked) | 112 | 60 |
| low-$\bar{X}_n$ | | |
| 6 wt %, 1K PDMS | 96 | 49 |
| 6 wt %, 5K PDMS | 102 | 55 |
| 6 wt %, 10K PDMS | 104 | 63 |
| 6 wt %, 20K PDMS | 106 | 63 |
| 20 wt %, 1K PDMS | 99 | 47 |
| 20 wt %, 5K PDMS | 106 | 64 |
| 20 wt %, 10K PDMS | 108 | 64 |
| 20 wt %, 20K PDMS | 109 | 65 |

All of the graft copolymers analyzed by TEM appeared to have a much higher volume fraction of the PDMS component than that calculated from the weight percent PDMS incorporated. This difference may be due to the altering of segmental densities brought about by the preferential solvation of the PDMS component during film formation. In addition, the overlap problem typically associated with interpreting two-dimensional TEM projections from three-dimensional objects makes it more difficult to accurately determine volume fractions by TEM. In order to clarify this situation, work is in progress by analyzing films cast from different solvents and by thermally annealing the samples to obtain equilibrium morphologies.

**Surface Analysis.** Because PDMS has a low surface energy relative to PBS and exists in a microphase-separated system, it was expected that the PDMS component would tend to dominate the air/solid interface of the copolymers.[29] Advancing and receding water contact angles were measured to verify these expectations, and the results are shown in Table VI. Water contact angle measurements indicated a change in the surface composition of the films as a function of copolymer composition and architecture. The graft copolymers prepared by using the high molar mass PDMS macromonomers, which phase separate to a higher degree, gave films exhibiting higher advancing water contact angles due to the presence of a more complete overlayer of the PDMS at the surface. This result agrees with several of our earlier studies with other related systems.[30]

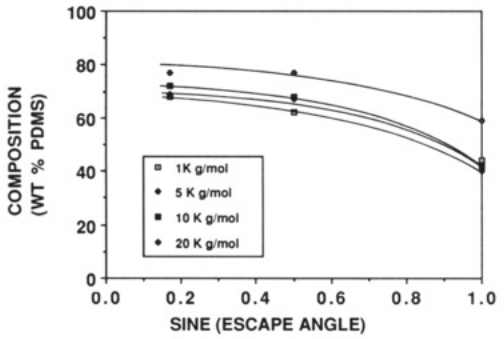


**Figure 9.** ADXPS data for 20 wt % PDMS, low-$\bar{X}_n$ PBS-*g*-PDMS copolymers plotted as a function of weight percent PDMS versus sine (escape angle).

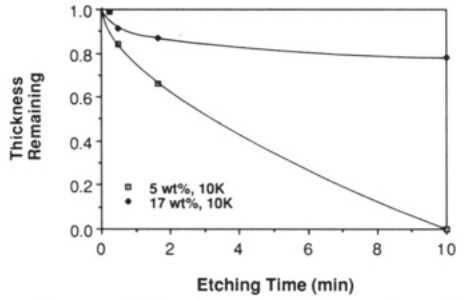


**Figure 10.** Oxygen RIE resistance data plotted as a function of normalized film thickness versus time in the RIE chamber for the high-$\bar{X}_n$ PBS-*g*-PDMS copolymers having 5 and 17 wt % PDMS with 10K g/mol PDMS grafts.

In order to quantify the surface composition, angular-dependent XPS was performed at angles of 15°, 30°, and 90° on solvent-cast samples. The higher angles of analysis penetrate deeper into the surface and reflect the composition average of approximately the top 60 Å at 90°, about 15 Å at 30°, and about 10 Å at a 10° angle. Angular-dependent XPS depth profiling indicated that the surface had a gradient of composition and that the surface composition was a function of copolymer composition and architecture. The data are presented as a plot of the detected composition versus the sine of the escape or sampling angle in Figure 9. Important trends in surface composition as a function of graft molar mass and depth are observed. It is evident that those copolymers having well-phase-separated bulk morphologies also exhibit significant surface segregation, which increases as the graft molar mass increases. The composition at the very top surface was found to be 4 times higher than the average bulk composition (determined by NMR and differential refractometry). This enhancement will play a dramatic role in the lithiographic performance of these materials as demonstrated in the next section.

**Lithographic Evaluation.** The resistance of the high-$\bar{X}_n$ PBS-*g*-PDMS copolymers to oxygen RIE was studied by using two series of copolymers having different chemical compositions, 5 and 17 wt % PDMS, respectively. Figure 10 is a plot of the normalized film thickness versus oxygen RIE time for two copolymers having the same molar mass PDMS graft (10K g/mol) but compositions of 5 and 17 wt % PDMS, respectively. At 5 wt % PDMS, resistance of PBS-*g*-PDMS to oxygen RIE is minimal whereas the 17 wt % PDMS graft copolymer exhibits superior resistance. The etch rate (measured at equilibrium between 100 and 600 s during analysis of a film with an initial thickness of 3200 Å) was 34 Å/min for the graft copolymer with 17 wt % PDMS. The etch rate of a hard-baked photoresist (HPR-204) under these conditions was 1000 Å/min. It has been reported that to avoid line-width erosion during RIE, it is necessary to have an etch rate ratio greater than 10:1 between the resist and the planarizing layer.[31] This corresponds to an etch rate ratio for the PBS-*g*-PDMS of 29:1, well within the regime for quality pattern transfer in two-layer lithography.

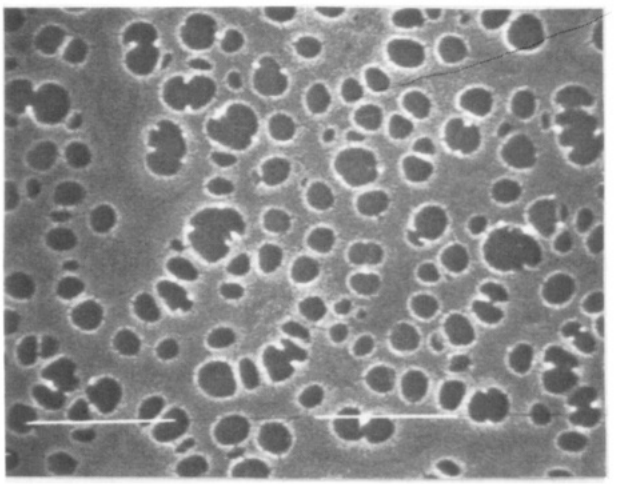

**Figure 11.** SEM of high-$\bar{X}_n$ PBS-*g*-PDMS copolymer having 5 wt % PDMS with 1K g/mol PDMS grafts after 10 min of oxygen RIE.

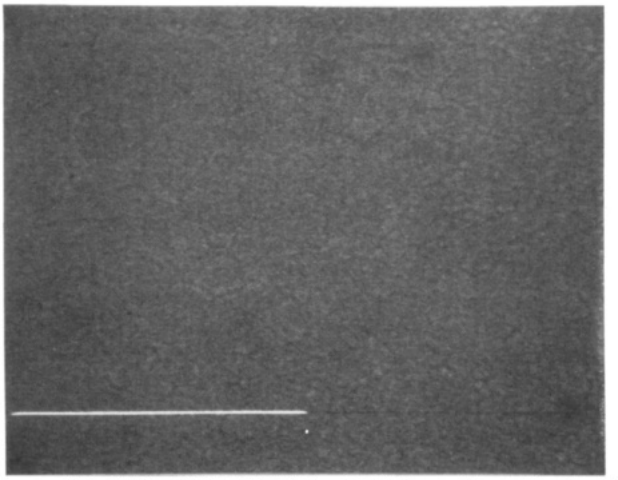

**Figure 12.** SEM of high-$\bar{X}_n$ PBS-*g*-PDMS copolymer having 17 wt % PDMS with 10K g/mol PDMS grafts after 10 min of oxygen RIE.

Figure 11 is a scanning electron micrograph (SEM) of the surface of the 5 wt % PDMS copolymer with 1K g/mol PDMS grafts after oxygen RIE exposure. The surface has considerable damage; several large craters are evident, reflecting the extensive degradation that has occurred. Figure 12 is an SEM of the 17 wt % PDMS copolymer having 10K g/mol grafts after a 10-min exposure to the oxygen RIE. The surface is essentially featureless at 100K magnification, reflecting the high stability of this material. XPS analysis of the samples after exposure to the oxygen RIE reveals that the binding energy of the silicon 2p electrons (103.3 eV) was indicative of silicon dioxide as opposed to PDMS for which the silicon 2p electrons have a binding energy of 102.4 eV. This result confirms that the mechanism for protection of the graft copolymers upon exposure to the oxygen RIE is the oxidative transformation of PDMS to silicon dioxide. Unlike poly(alkenylsilane sulfone)s, the 17 wt % PDMS graft copolymers did not require special surface passivation treatment prior to "normal" RIE processing.[32] The high resistance of this material is interesting in that it only contains 6.4 wt % silicon whereas previously published results imply that at

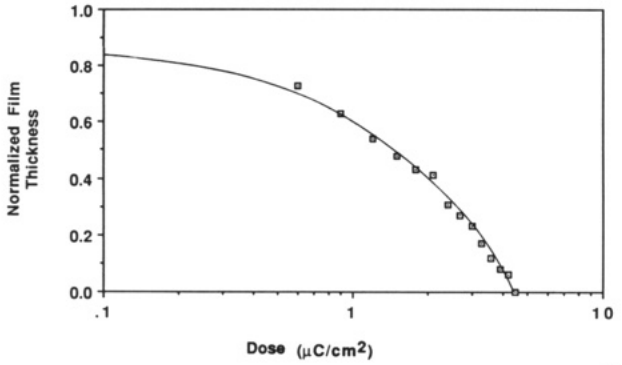


**Figure 13.** Electron beam sensitivity curve PDMS of high-$\bar{X}_n$ PBS-*g*-PDMS copolymer having 17 wt % PDMS with 10K g/mol PDMS grafts for development in 5-methyl-2-hexanone.

least 8–12 wt % silicon is required to impart sufficient resistance to oxygen RIE.[8c] The high resistance of the graft copolymer having 17 wt % PDMS to oxygen RIE may be directly related to two factors. First, the reported value of 8–12 wt % silicon was based on polymers containing trialkylsilicon moieties, not siloxane units that contain silicon already bonded to two oxygen atoms. Second, it was demonstrated on films formed by slow evaporation that the surface of the copolymers was rich in the PDMS component. The silicon concentration at the solid/gas interface actually approaches 30 wt % (or 80 wt % PDMS) according to the ADXPS data. Since the protective mechanism is a surface phenomenon, perhaps the materials are above a critical threshold of silicon concentration where it is most important, at the top few nanometers of the surface.

The high-$\bar{X}_n$ PBS-*g*-PDMS copolymer containing 17 wt % PDMS and having 10K g/mol PDMS grafts was selected for preliminary lithographic sensitivity evaluation. The sensitivity, determined as the *x* axis intercept in the sensitivity curve shown in Figure 13 for a 30-s development in 5-methyl-2-hexanone, was ca. 4.5 $\mu$C/cm$^2$ at 25 kV, which is similar to that of the PBS homopolymer. Some thinning of the resist took place during this development procedure (contrast <2), and it is anticipated that, in conjunction with optimization of the development procedure, copolymers with even higher degrees of polymerization would diminish this problem.

The lithographic potential of the copolymers was demonstrated by transferring a high-density periodic pattern through the resist to the 1.2-$\mu$m-thick novolac substrate in a two-layer test sample (Figure 14). The SEMs show that good resolution was obtained for 0.2-$\mu$m lines with a 0.4-$\mu$m pitch, resulting in a >4.5 aspect ratio.

## Conclusions

The 5-hexenyl functional end group of the PDMS macromonomers allows the incorporation of PDMS graft segments into PBS. The PDMS macromonomers can be synthesized to have controlled molar masses, narrow molar mass distributions, and high percent functionalities. These are important parameters that have allowed the elucidation of the structure/property relationships in graft copolymers of poly(1-butene sulfone). The graft copolymers exhibited microphase-separated morphologies, as determined by DSC and TEM, that varied as the architecture and the composition of the copolymers were changed. The degree of microphase separation was found to increase as the graft molar mass increased at constant composition. The low surface energy component, PDMS, was found to dominate the air/solid interface as determined by water contact angle measurements and ADXPS. Enhancement

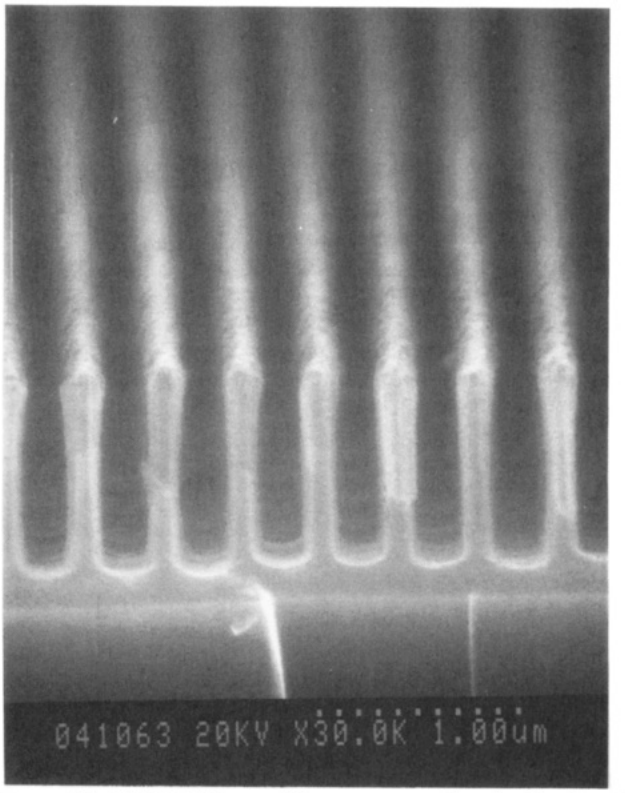


**Figure 14.** SEM of lithographic patterns produced using the 17 wt % PDMS high-$\bar{X}_n$ PBS-*g*-PDMS copolymer as a resist in a bilayer structure with a 1.2-$\mu$m-thick novolac planarizing layer. The sample was exposed with 3.5 $\mu$C/cm$^2$ of electron beam irradiation at 50 kV, followed by a 30-s dip development in 5-methyl-2-hexanone, and the pattern was transferred by 14 min of oxygen RIE.

of the surface by PDMS was shown to be a function of the average chemical composition and architecture of the copolymer. Copolymers containing 17 wt % PDMS exhibited superior resistance to oxygen RIE processes without prior passivation of the surface. In addition, preliminary lithographic sensitivity and contrast data indicate that the lithiographic properties are similar to those of the PBS homopolymer. The combination of high resistance to oxygen RIE and high sensitivity to electron beam exposure may allow this new class of resist material to function as a fast electron beam resist for the direct-write fabrication of lithographic devices.

**Acknowledgment.** We thank Dr. Paul S. D. Lin and Bart van der Gaag of Bellcore for the electron beam exposures and Professor H. Marand for his helpful discussions concerning the DSC work. In addition, the authors from VPI thank Bellcore for partial funding for this project and Professor Kratochvil and his co-workers for the isorefractive light scattering data.

## References and Notes

(1) Fawcett, A. H. In *Encyclopedia of Polymer Science and Engineering*; Kroshwitz, J. I., Ed.; Wiley: New York, 1987; pp 408–432.
(2) Brown, J.; O'Donnell, J. H. *Macromolecules* **1970**, *3*, 265.
(3) Bowden, M. J.; Thompson, L. F. *J. Electrochem. Soc.* **1973**, *120*, 1722.
(4) Slemp, W. S.; Santos-Mason, B.; Sykes, G. F.; Witte, W. G. AIAA 23rd Aerospace Meeting, Jan 1985, AIAA-85-0421.
(5) Visentine, J. T.; Lejer, L. J.; Kuminecz, J. F.; Spiker, I. K. AIAA 23rd Aerospace Meeting, Jan 1985, AIAA-85-0415.
(6) Johnson, B. C. Ph.D. Dissertation, Virginia Polytechnic Institute and State University, 1983. Summers, J. D. Ph.D. Dissertation, Virginia Polytechnic Institute and State University, 1987.

(7) Arnold, C. A.; Chen, D.; Chen, Y. P.; Graybeal, J. D.; Bott, R. H.; Yoon, T.; McGrath, B. E.; McGrath, J. E. *PMSE Prepr. (Am. Chem. Soc., Div. Polym. Mater. Sci. Eng.)* **1988**, *59*, 934. Arnold, C. A.; McGrath, J. E. Materials Research Society Symposium, San Diego, April 1989.
(8) Reviews: (a) Lin, B. J. Multilayer Resist Systems. *Introduction to Microlithography*; Thompson, L. F., Willson, C. G., Bowden, M. J., Eds.; ACS Symposium Series 219; American Chemical Society: Washington, DC, 1983; p 304. (b) Hatzakis, M. *Solid State Technol.* **1981**, *24*, 74. (c) Reichmanis, E.; Smolinsky, G.; Wilkens, C., Jr. *Solid State Technol.* **1985**, *28*, 130. (d) McDonnell Bushnell, L. P.; Gregor, L. V.; Lyons, C. F. *Solid State Technol.* **1986**, *29*, 133.
(9) Gozdz, A. S.; Carnazza, C.; Bowden, M. J. *Proc. SPIE* **1986**, *631*, 2.
(10) Ito, S.; Ono, H.; Kim, S. J.; Matsuda, M. IUPAC, 32nd International Symposium on Macromolecules, Aug 1988, Paper 4-8-17, p 542.
(11) Gozdz, A. S.; Ito, S.; Ono, H.; Shelburne, J. A.; Matsuda, M. *Proc. SPIE*, in press.
(12) Bowden, M. J.; Gozdz, A. S.; Klausner, D.; McGrath, J. E.; Smith, S. D. In *Polymers for High Technology: Electronics and Photonics*; Bowden, M. J., Turner, R. S., Eds.; ACS Symposium Series 346; American Chemical Society: Washington, DC, 1987; pp 122–137.
(13) DeSimone, J. M.; Smith, S. D.; McGrath, J. E. *Polym. Prepr. (Am. Chem. Soc., Div. Polym. Chem.)* **1988**, *29* (2), 345.
(14) Lebedev, B. B.; Mukhina, N. N.; Kulagina, T. G. *Polym. Sci. USSR (Engl. Transl.)* **1979**, *20*, 1458.
(15) Wang, B.; Krause, S. *Macromolecules* **1987**, *20*, 2201.
(16) Winstein, S.; CLippinger, E.; Fainberg, A. H.; Heck, R.; Robinson, G. C. *J. Am. Chem. Soc.* **1956**, *78*, 328.
(17) Wilczek, L.; Kennedy, J. P. *Polym. J.* **1987**, *19* (5), 531.
(18) Lee, C. L.; Frye, C. L.; Johannson, O. K. *Polym. Prepr. (Am. Chem. Soc., Div. Polym. Chem.)* **1969**, *10* (2), 361.
(19) Bostick, E. E. In *Block Copolymers*; Aggarwal, S. L., Ed.; Plenum: New York, 1970; pp 237–247.
(20) Saam, J. C.; Gordon, D. J.; Lindsey, S. *Macromolecules* **1970**, *3*, 1308.
(21) Fessler, W.; Juliano, P. C. *Ind. Eng. Chem. Prod. Res. Dev.* **1972**, *11* (4), 407.
(22) Yamashita, Y. *J. Appl. Polym. Sci., Appl. Polym. Symp.* **1981**, *36*, 193.
(23) Kawakami, Y.; Murhty, R. A. N.; Yamashita, Y. *Makromol. Chem.* **1984**, *185*, 9.
(24) Riffle, J. S.; Sinai-Zingde, G.; DeSimone, J. M.; Hellstern, A. M.; Chen, D. H.; Yilgor, I. *Polym. Prepr. (Am. Chem. Soc., Div. Polym. Chem.)* **1988**, *29* (2), 93.
(25) Smith, S. D. Ph.D. Dissertation, Virginia Polytechnic Institute and State University, 1987.
(26) Ito, K.; Tsuchida, H.; Kitano, T. *Polym. Bull.* **1986**, *15*, 425.
(27) Analysis was kindly performed in Professor Kratochvill's laboratory in Prague. For a description of the analyses, see: Stejskal, J.; Strakova, D.; Kratochvil, P.; Smith, S. D.; McGrath, J. E. *Macromolecules* **1989**, *22*, 861.
(28) Lee, C. L.; Johannson, O. K.; Flanningam, O. L.; Hahn, P. *Polym. Prepr. (Am. Chem. Soc., Div. Polym. Chem.)* **1969**, *10*, 1311.
(29) Patel, N. M.; Dwight, D. W.; Hedrick, J. L.; Webster, D. C.; McGrath, J. E. *Macromolecules* **1988**, *21*, 2689.
(30) Smith, S. D.; DeSimone, J. M.; York, G. A.; Dwight, D. W.; Wilkes, G. L.; McGrath, J. E. *Polym. Prepr. (Am. Chem. Soc., Div. Polym. Chem.)* **1987**, *28* (2), 150.
(31) Tarascon, R. G.; Shugard, A.; Reichmanis, E. *Proc. SPIE, Adv. Resist Technol. Process. III* **1986**, *631*, 40.
(32) Gozdz, A. S.; Carnazza, C.; Bowden, M. J. *Proc. SPIE, Adv. Resist Technol. Process. III* **1986**, *631*, 2.

**Registry No.** $(H_2C{=}CH(CH_2)_2H)(SO_2)(D_3)$ (copolymer), 124659-77-4.